Communications Research Centre

COMPARISONS OF THE DETECTION PERFORMANCE OF A SPACE-BASED RADAR SYSTEM USING DIFFERENT ANTENNA SYSTEMS AND APERTURE ILLUMINATIONS

by

B.J. Rook

This work was sponsored by the Department of National Defence, Research and Development Branch under Project No. 33C87.

CRC REPORT NO. 1401
OTTAWA, MAY 1986

Canada

COMMUNICATIONS RESEARCH CENTRE

DEPARTMENT OF COMMUNICATIONS
CANADA

COMPARISONS OF THE DETECTION PERFORMANCE OF A SPACE-BASED RADAR SYSTEM USING DIFFERENT ANTENNA SYSTEMS AND APERTURE ILLUMINATIONS

by

B.J. Rook

(Radar and Communications Technology Branch)

CRC REPORT NO. 1401

May 1986
OTTAWA

This work was sponsored by the Department of National Defence, Research and Development Branch under Project No. 33C87.

TABLE OF CONTENTS

COMPARISONS OF THE DETECTION PERFORMANCE OF A SPACE-BASED RADAR SYSTEM USING DIFFERENT ANTENNA SYSTEMS AND APERTURE ILLUMINATIONS

ABSTRACT

Comparisons have been made of the results of the detection performance of a space-based radar (SBR) system using uniformly-illuminated circular apertures, and the same apertures with Taylor weighting applied. From the studies, it is shown that the detection performance of an SBR system can be greatly improved with the application of the latter form of weighting.

For the comparative studies, two antenna systems with the same physical dimensions were used, (1) a Taylor-weighted circular aperture for transmitting and receiving, and (2) a uniformly-illuminated circular aperture for transmitting, and the same aperture but with Taylor weighting applied for receiving. These comparative studies show that when antenna system (1) was used, 45.0 dB Taylor weighting was required in order to achieve the optimum SBR detection performance whereas for antenna system (2), 55.0 dB was required to give the same detection performance.

1. INTRODUCTION

The detection of targets near the surface of the Earth by an SBR system is difficult because radar echoes from the target are immersed in clutter echoes from the surface of the Earth. The latter can be very large because of the relatively large footprint of the antenna pattern, and the unwanted contributions of earth clutter entering through the sidelobes, particularly those adjacent to the main lobe. Aperture weighting is used to reduce these sidelobes to a sufficiently low level in order to suppress the earth-clutter returns.

There are numerous types of aperture weighting, and in this report consideration is given to Taylor weighting. The advantage of using Taylor weighting for this application is that the sidelobes may be reduced to a uniform design level within a specified angular region from the main lobe. Beyond this angular region the sidelobe levels decrease with increasing angle.

In this report, results are presented of the detection performance of an SBR system using an antenna system comprising a Taylor-weighted circular aperture for transmitting and receiving, using different design sidelobe-level ratios. These results are compared with the results of the detection performance of an antenna system comprising a uniformly-illuminated circular aperture on transmit and the same aperture but with Taylor weighting applied on receive. In these comparative studies, the same physical aperture dimensions were employed for both antenna systems. The candidate SBR system used for the studies is the simulated baseline system described in [1], which employs the uniformly-illuminated circular aperture on transmit and receive. Included in the simulator is a model of the earth-clutter returns. A brief description of the baseline system is given in Section 5.

2. DESCRIPTION OF THE COORDINATE SYSTEMS

In this section, a description is given of the coordinate systems that are used for calculating the look-direction to the target from the radar satellite, and for calculating the off-axis beam response of the radar-satellite antenna.

2.1 Description of the North-East-Down Coordinate System

In this sub-section, a description is given of the coordinate system that is used in calculating the look-direction to the target from the radar satellite. This system, which is centred at the satellite, is illustrated in Fig.(1). The various symbols in this figure are defined as follows:-

s is the instantaneous position of the satellite;

δ_s is the lattitude of the satellite measured from the equatorial plane;

r is the radial distance of the satellite measured from the centre of the Earth denoted by F;

R is the slant or radar range to the target T which is assumed to be located on or near the surface of the Earth.

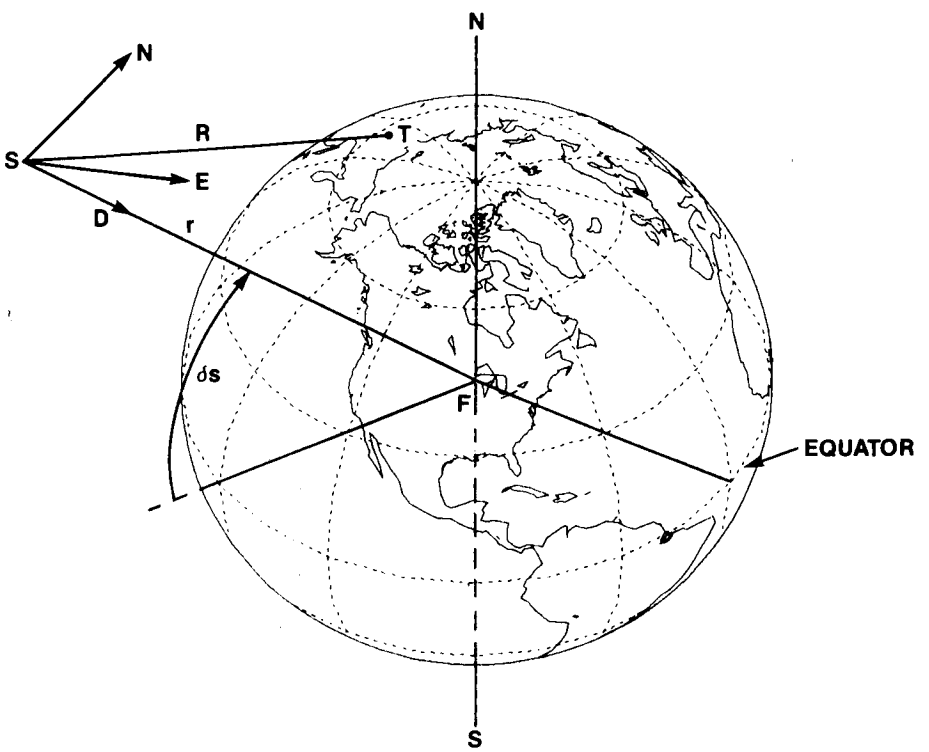

Figure 1 Illustration of the Satellite-target geometry in the Satellite's local north-east-down (N,E,D) coordinate system.

The coordinate system used is the north-east-down (N,E,D) system with its origin at s as shown in the diagram. The N-coordinate is directed toward the geometric north pole; the E-coordinate is directed perpendicularly outwards from the N-coordinate in an easterly direction. These two coordinates define the north-east (N-E) plane. The third coordinate, denoted D, is directed perpendicularly downwards from the N-E plane along the radial distance r. The look-direction to the target in spherical coordinates (θ_L, ϕ_L) may be determined from the projections along the N,E and D coordinates. The angle θ_L, defined as the look-down angle, is measured from the N-E plane, and the angle ϕ_L, defined as the look-azimuth angle, is measured east of north. These spherical coordinates are illustrated in fig.(1a).

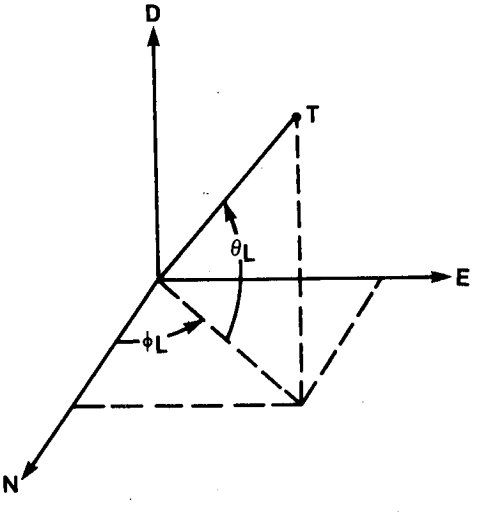

Figure 1a Illustration of the N,E,D system defining θ_L, ϕ_L.

An angle which is used extensively in Section 6 of this report is the grazing angle γ. This angle is measured from a line tangent to the Earth's surface at T, to the slant range R. Its relationship with θ_L, R and r is illustrated in fig.(2). Their mathematical relationships may be determined from this geometry, and are given by the following geometrical identities:-

$$\frac{\sin(\theta_L-\gamma)}{R} = \frac{\cos\theta_L}{r_e} = \frac{\cos\gamma}{r} \qquad (1)$$

where r_e is the radius of the Earth normally taken to be $6.378\text{x}10^6$ metres. By inspection of fig.(2) or eqn.(1), it is noted that the grazing angle ranges from $0 \leq \gamma \leq \pi/2$ whereas the corresponding angles for θ_L range from a minimum value dependent on the altitude of the satellite to a maximum value of $\pi/2$. Thus for the results given in Section 6, γ is used in place of θ_L in specifying the look-direction, since the range of γ is always the same regardless of the altitude of the satellite.

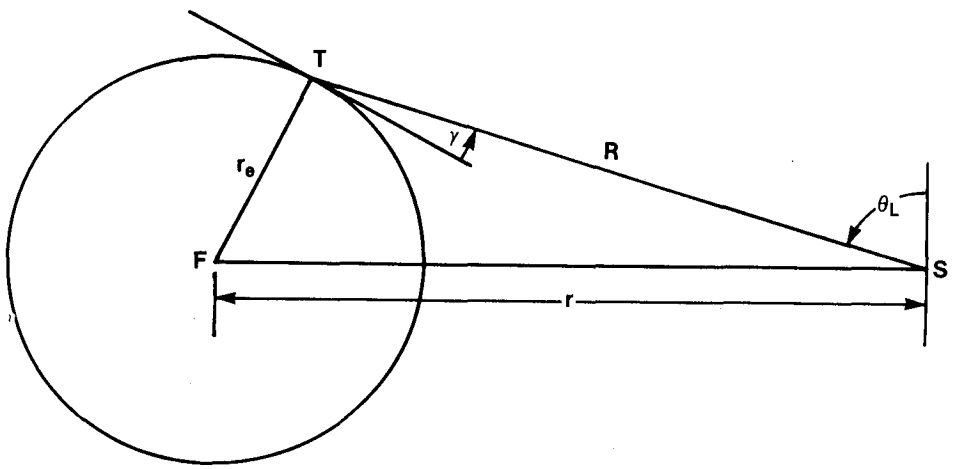

Figure 2 Diagram of the earth-satellite geometry illustrating the relationship of γ with θ_L, r and R.

2.2 Relationship Between the Aperture Coordinate System and the N,E,D System

In fig.(3), an illustration is given of the relationship between the N,E,D coordinate system and the x,y,z aperture coordinate system, where the origin of both systems are the same. The z-coordinate is

directed perpendicularly outwards from the plane of the antenna aperture (here, depicted as a circular aperture) along the slant range R to the target. The x and y coordinates are in the plane of the aperture as shown. In this way, the antenna always presents maximum aperture to the target since it is always assumed to be oriented in the look-direction (θ_L, ϕ_L). Thus, for any arbitrary θ and ϕ, the projections along the x, y and z coordinates, namely x_1, y_1 and z_1 are determined by a coordinate transformation from the N,E,D system into the x,y,z system from which the off-axis antenna beam response is calculated. These projections are given from [1] as

$$x_1 = \sin\theta_L \cos\theta \cos(\phi - \phi_L) - \cos\theta_L \sin\theta \quad , \tag{2}$$

$$y_1 = \cos\theta \sin(\phi - \phi_L) \tag{3}$$

and

$$z_1 = \cos\theta_L \cos\theta \cos(\phi - \phi_L) + \sin\theta_L \sin\theta \quad . \tag{4}$$

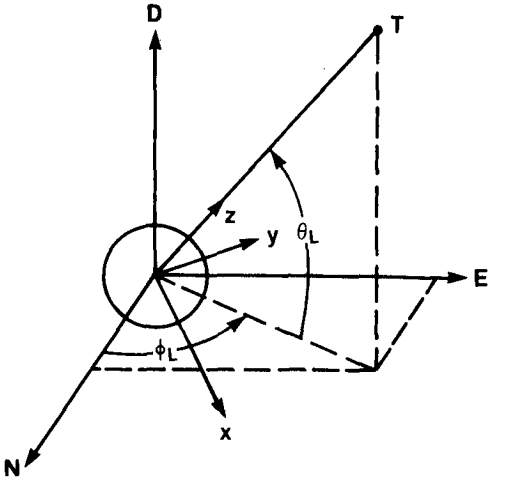

Figure 3 Relationship between the north-east-down (N,E,D) coordinate system and the antenna aperture (x,y,z) coordinate system.

In the following section, it will be shown how these projections are used in calculating the antenna responses for the uniformly-

illuminated circular aperture, and the same aperture but with Taylor weighting applied.

3. TAYLOR CIRCULAR APERTURE AND EXCITATION EFFICIENCY

Low sidelobes and narrow beam arrays may be designed by the Dolph-Tchebyscheff process. This process produces an optimum antenna pattern in that it gives an optimum beamwidth to sidelobe-level relationship for a given design sidelobe-level ratio. In the limit, as the number of elements approach infinity in a given Dolph-Tchebyscheff array size, the optimum pattern approaches the ideal[2] pattern giving an infinite number of sidelobes all with the same design level. However, this ideal antenna pattern is not physically realizeable because the currents in the end elements of the aperture become very large compared with the currents in the rest of the elements, and the ideal pattern becomes very sensitive to changes in the excitation at the end elements. This sets an upper limit of the number of elements that can be used in a Dolph-Tchebyscheff array, and sets a lower limit to the width of the main beam that can be achieved.

To realize a physical approximation to the ideal antenna pattern of a Dolph-Tchebyscheff array using large numbers of elements, Taylor[3,4] modified the corresponding aperture distribution to produce an antenna pattern with equal sidelobes out to a point beyond which the sidelobe amplitude decreases. The currents in the end elements of the array can be adjusted by moving this transition point.

In this section, formulae are developed to synthesize the normalized antenna power response of a circular aperture when Taylor weighting is applied, and to compute the corresponding aperture distribution and excitation efficiency. Results are then presented to illustrate Taylor circular-aperture distributions and excitation efficiencies for different values of the sidelobe-level ratio. In addition, graphical results are presented to compare the normalized antenna responses of the Taylor-weighted and uniformly-illuminated circular apertures.

Using the coordinate system described in Section 1, the normalized antenna power response for a uniformly-illuminated circular aperture is given from [1] as

$$G_c(\theta,\phi) = \left[\frac{2J_1(\pi u)}{\pi u} \right]^2 \tag{5}$$

where $J_1(X)$ is a first-order Bessel function, and u is given by

$$u = \frac{2a}{\lambda} (x_1^2 + y_1^2)^{\frac{1}{2}} \tag{6}$$

where a is the radius of the aperture and λ is the radar wavelength, and where the variables x_1 and y_1 are the projections along the x and y coordinates of the (x,y,z) aperture coordinate system given by eqns.(2) and (3) respectively. Thus, for the specified look-direction (θ_L, ϕ_L) along which the boresight of the aperture is directed, eqn.(5) gives the normalized off-axis beam response in the arbitrary look-direction θ, ϕ.

The antenna power pattern of a Taylor-weighted circular aperture takes on the form[5]

$$G_c^T(\theta,\phi) = \left[\frac{2J_1(\pi u)}{\pi u} \prod_{n=1}^{\bar{n}-1} \frac{1 - (u/z_n)^2}{1 - (u/u_n)^2} \right]^2 \tag{7}$$

where u_n are the values at which $J_1(\pi u_n) = 0$, several of which are given in Table 1,

TABLE 1

Solutions of $J_1(\pi u_n) = 0$

n	u_n
1	1.2197
2	2.2331
3	3.2383
4	4.2411
5	5.2428
6	6.2439
7	7.2448
8	8.2454
9	9.2459
10	10.2463

and where

$$\left.\begin{aligned} z_n &= \pm\sigma\left[A^2 + (n - \tfrac{1}{2})^2\right]^{\frac{1}{2}} && 1 \le n < \bar{n} \\ z_n &= \pm u_n && \bar{n} \le n < \infty \end{aligned}\right\} \qquad (8)$$

and

$$\sigma = u_{\bar{n}} / \left[A^2 + (\bar{n} - \tfrac{1}{2})^2\right]^{\frac{1}{2}} \qquad (9)$$

In eqns.(8) and (9) the parameter A is used to control the sidelobe-level ratio (SLR). The relationship between A and the SLR is given by

$$\mathrm{SLR} = \cosh \pi A \qquad (10)$$

The parameter σ given by eqn.(9) and used in eqn.(8) is a stretching factor which causes the distances between the zeros of the function $G_c^T(\theta,\phi)$ to be stretched slightly relative to those of the function $G_c(\theta,\phi)$ out to the values $\pm u_{\overline{n}}$ where the zeros of both functions occur at $J_1(\pi u_{\overline{n}}) = 0$. Thus, the procedure keeps the near-in sidelobe at or below the designed level out to $\pm u_{\overline{n}}$ beyond which the sidelobe levels decrease.

The beamwidth of a Taylor-weighted circular aperture is given by[4]

$$\beta = \frac{\sigma \beta_o \lambda}{2a} \tag{11}$$

where β_o is the beamwidth of the ideal antenna pattern in units of standard beamwidths, where $\lambda/2a$ is a standard beamwidth. An expression for β_o is given by the following equation:

$$\beta_o = \frac{2}{\pi} \left\{ \left[\cosh^{-1}(SLR)\right]^2 - \left[\cosh^{-1}(SLR/\sqrt{2})\right]^2 \right\}^{\frac{1}{2}} . \tag{12}$$

The aperture distribution is given from Taylor[4] as

$$g(P) = \frac{2}{\pi^2} \sum_{m=0}^{\overline{n}-1} \frac{F(u_m,A,\overline{n})\ J_o(u_m P)}{\left[J_o(\pi u_m)\right]^2} \tag{13}$$

where $J_o(X)$ is a zero-order Bessel function and the radial variable $P = \pi p/a$, where the p variable is the measured radial distance from the centre of the aperture. The coefficient $F(u_m,A,\overline{n})$ is equal to unity for $m = 0$, and for $m > 0$ is equal to

$$F(u_m,A,\bar{n}) = -J_o(\pi u_m)\ \frac{\prod_{n=1}^{\bar{n}-1}\left[1 - u_m^2/\sigma^2[A^2+(n-\frac{1}{2})^2]\right]}{\prod_{\substack{n=1\\ n\neq m}}^{\bar{n}-1}\left[1 - u_m^2/u_n^2\right]} \qquad (14)$$

The aperture excitation efficiency η, that is, the ratio of the directive gain of an antenna with a weighted aperture relative to that which is uniformly-illuminated, is given from [5] for a Taylor circular distribution as

$$\eta = \frac{2\left(\int_o^\pi g(P)PdP\right)^2}{\pi^2\int_o^\pi g^2(P)PdP} \qquad (15)$$

Rudduck et al[6] have shown that when the integration is performed in eqn.(15), the result reduces to

$$\eta = \frac{1}{1 + \sum_{n=1}^{\bar{n}-1}\frac{F(u_n,A,\bar{n})}{J_o^2(\pi u_n)}} \qquad (16)$$

At this point, it is necessary to discuss the appropriate range of $\bar{n}$. Too large a value of $\bar{n}$ will produce large peaks in the distribution at the ends of the aperture similar to the Dolph-Tchebyscheff distribution for large numbers of elements. On the other hand, too small a value will not allow the transition-zone zeros of the antenna pattern to behave properly and as a result, the designed SLR will not be realized. A reasonable value for this parameter is the maximum value for $\bar{n}$ that will allow a monotonically decreasing aperture function. This value may be regarded as optimum since the corresponding antenna response is not influenced by changes in the excitation at the end elements. However, the value is not optimum where excitation efficiency

is concerned, since a larger value of $\bar{n}$ is required for the excitation efficiency to maximize.

In fig.(4), plots are given of the aperture distribution using the maximum value of $\bar{n}$ that will allow a monotonically decreasing aperture function. The maximum $\bar{n}$ are $\bar{n} = 5$ for SLR = 30.0 dB, $\bar{n} = 8$ for SLR = 40.0 dB, and $\bar{n} = 11$ for SLR = 50.0 dB. Only half of each aperture distribution is plotted since each distribution is symmetrical about the centre.

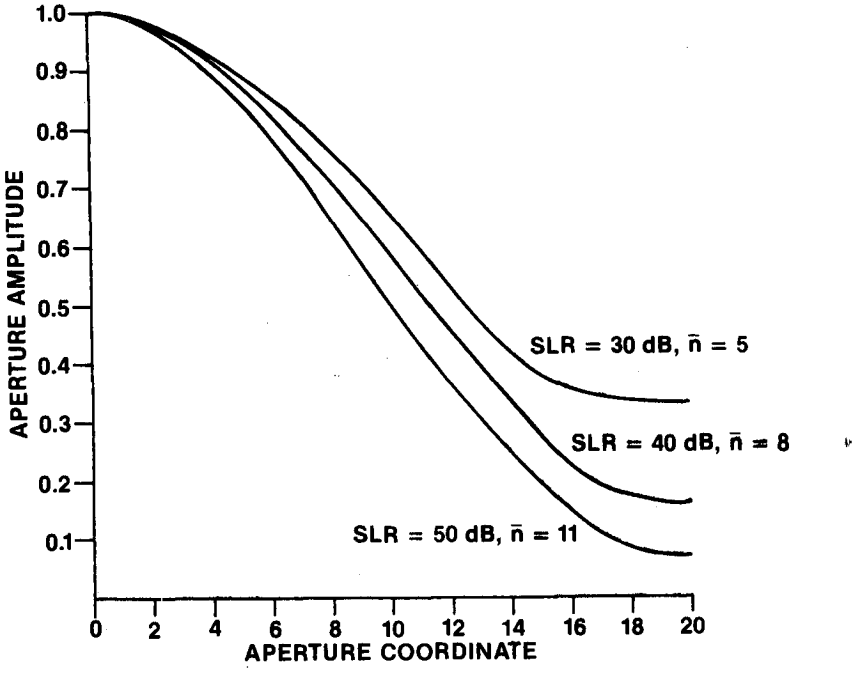

Figure 4 Plots of a Taylor-weighted circular aperture distribution for the values of SLR and $\bar{n}$ as shown.

In fig.(5), a comparison is made of the aperture functions corresponding to (1) a 40.0 dB Taylor distribution using a $\bar{n} = 21$ to give the maximum aperture efficiency, and (2) a 40.0 dB Taylor distribution using the largest value of $\bar{n}$ which will yield a monotomically decreasing function. Note that the illumination function for (1) is peaked at the edge and has a local minimum. This type of

illumination function is usually considered impractical to implement. For this reason, and noting that aperture efficiency is an increasing function of $\bar{n}$, the best design choice is the largest value of $\bar{n}$ that will still give a monotonically decreasing aperture illumination function.

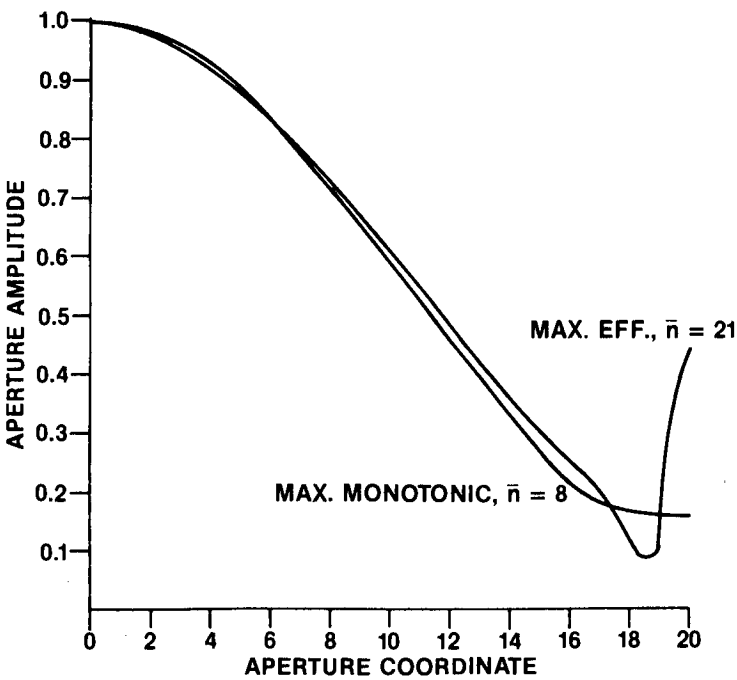

Figure 5 Plots of the $\bar{n}$ Taylor distributions for SLR = 40.dB

In Table 2, results are given of the efficiencies and corresponding $\bar{n}$ values for non-monotonically decreasing aperture functions for comparisons with those that use the largest $\bar{n}$ while still having a monotonically decreasing aperture function. Note that the differences in the efficiency values are small.

TABLE 2

Taylor $\bar{n}$ Distributions

Max η values			Monotonic $\bar{n}$	
SLR(dB)	$\bar{n}$	η	$\bar{n}$	η
30	8	0.8839	5	0.8623
40	21	0.7584	8	0.7252
50	50	0.6449	11	0.6106

In Table 3, values are given for the parameters A^2 and σ for different values of the design sidelobe-level ratio (SLR) and $\bar{n}$ which give monotonically decreasing aperture distributions. Corresponding values for β_o and η are also given together with corresponding values for $\sigma\beta_o$ in terms of a standard beamwidth. It may be noted that the aperture excitation efficiency decreases with increasing SLR, and that $\sigma\beta_o$ increases with increasing SLR. In the results to be presented in Section 6, Taylor $\bar{n}$ monotonic distributions are considered using different design sidelobe-level ratios and related excitation efficiencies given in this table. The corresponding antenna responses are computed from eqns.(7) - (9) using the corresponding parameters in the table.

TABLE 3

Taylor $\bar{n}$ Monotonic Distributions						
SLR (dB)	$\bar{n}$	A^2	σ	β_o	η	$\sigma\beta_o$
30	5	1.7425	1.1180	1.0566	0.8623	1.1813
40	8	2.8443	1.0726	1.1999	0.7252	1.2870
45	10	3.4959	1.0583	1.2655	0.6663	1.3393
50	11	4.2147	1.0512	1.3279	0.6106	1.3959
55	15	5.0006	1.0393	1.3874	0.5689	1.4419
60	16	5.8537	1.0357	1.4445	0.5265	1.4961

In fig.(6) the solid line shows a plot of the normalized antenna power pattern as a function of u for the circular aperture when 40.0 dB Taylor weighting is applied with $\bar{n} = 8$. For comparison, the dashed line shows the normalized antenna power pattern of a uniformly-illuminated circular aperture of the same size. This pattern has a maximum sidelobe level of 17.5 dB below the main lobe. It is noted that the Taylor-weighted aperture has reduced the corresponding sidelobes of the antenna pattern to 40.0 dB relative to the main lobe, but the main lobe has increased in comparison to that of the uniformly-illuminated aperture. Thus, with the application of aperture weighting, the sidelobes may be reduced to a designed SLR, but at the expense of broadening of the main lobe and a reduction in the excitation efficiency.

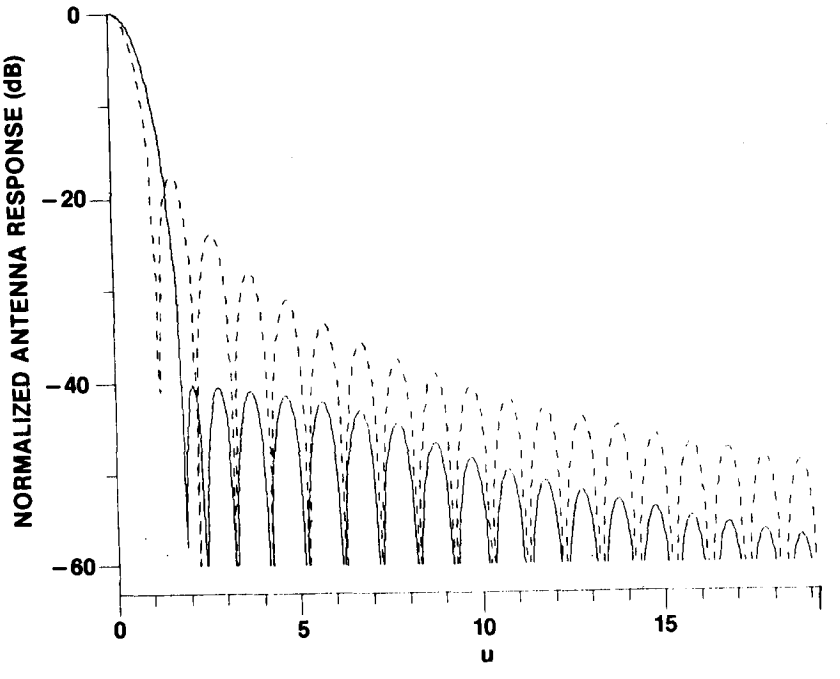

Figure 6 Antenna power response for a 40.0 dB Taylor-weighted circular aperture, $\bar{n} = 8$

4. PEAK-POWER SCALE FACTOR

In the previous section, it was shown that with the application of Taylor weighting to the circular apertures, the directive gain of the antenna decreased relative to that which is uniformly-illuminated. This relationship was quantified by the aperture excitation efficiency η. In this section, an adjustment factor will be derived to compensate for different antenna aperture sizes and excitation efficiencies so that the power density at the maximum of the antenna pattern is the same for all antenna systems to be compared in the baseline system. This adjustment factor is called the peak-power scale factor and is used to adjust the radar's peak power for the antenna system being compared.

In the SBR baseline system, the product of the two-way maximum antenna gain G_c^2 for the uniformly-illuminated circular aperture, and the peak power P_k is constrained to equal a constant value K:

$$P_k G_c^2 = K \quad , \tag{17}$$

and

$$G_c = \frac{4\pi\eta_c A_c}{\lambda^2} \tag{18}$$

where A_c is its physical area, λ is the wavelength, and η_c is the aperture excitation efficiency which is unity for this aperture. If this antenna system is replaced by another antenna system for a comparison of the detection performance, we have that

$$PG_T G_R = P_k G_c^2 = K \tag{19}$$

where G_T is the maximum gain of the transmitting antenna, G_R is the maximum gain of the receiving antenna, and P is the peak power required for the replaced antenna system. Here, a general situation has been taken where the transmitting antenna may not necessarily have the same characteristics as the receiving antenna. Thus, rearranging eqn.(19) to solve for P gives

$$P = \left(\frac{G_c^2}{G_T G_R} \right) P_k = \left(\frac{A_c^2}{\eta_T A_T \eta_R A_R} \right) P_k \tag{20}$$

The factors inside the parenthesis in eqn.(20) constitutes the peak-power scale factor (PF) which, when multiplied by P_k, gives the peak power required of the radar for the selected antenna system.

In the following sections, two antenna systems will be used in the SBR system for a comparison of the detection performance. These two systems are:

(1) Taylor-weighted circular aperture for transmitting and receiving;

(2) Uniformly-illuminated circular aperture for transmitting and a Taylor-weighted circular aperture for receiving.

It is assumed that both these antenna systems have the same physical aperture dimensions. If antenna system (1) is used, then $A_C = A_T = A_R$, and $\eta_T = \eta_R = \eta^2$, therefore, the peak-power scale factor (PF) for this system is

$$PF_{(1)} = 1/\eta^2 \quad . \tag{21}$$

If antenna system (2) is used, then $A_C = A_T = A_R$, and $\eta_T = 1$, therefore, the peak-power scale factor (PF) for this system is

$$PF_{(2)} = 1/\eta_R = 1/\eta \quad . \tag{22}$$

The result of eqn.(21) indicates that the peak power increases as the reciprocal of the square of the excitation efficiency for antenna system (1). The result of eqn.(22) indicates that the peak-power increases only as the reciprocal of the excitation efficiency for antenna system (2). By a comparison of these two results, there is an advantage in using a uniformly-illuminated aperture for transmitting, and the same aperture but with Taylor weighting applied for receiving, if there are constraints to the peak power available on-board a radar satellite. However, this factor should be weighed against other factors such as the relative performance of the two systems, which is discussed in Section 6, and the difficulty of implementing a carefully controlled taper of the transmit illumination function, in determining the relative merits of one system over another.

5. DESCRIPTION OF THE SBR BASELINE SYSTEM

In this section, a description is given of the SBR baseline system which is to be used for the comparative studies of the detection performance using the antenna systems previously described.

An L-band radar satellite ($\lambda = 0.2$m) at an altitude of 1000 Km above the surface of the Earth and operating in a circular-polar orbit is the baseline system used[1]. The objective for the system is to detect

a near-earth target having a radar cross-section σ_T of -10.0 dBsm with a probability of detection of 0.9 and a false alarm probability of less than 10^{-6}. This value for σ_T is chosen to reflect what might be considered as a lower limit of target cross-sections for detection by the radar satellite. With these detection and false alarm probabilities and assuming two bursts are noncoherently added, the signal-to-interference ratio must be 14.8 dB. This value is obtained from Swerling's case 2 for fluctuating targets where the two bursts are at different radar frequencies. Adding 3 dB to take account of cusping losses gives a minimum designed signal-to-interference ratio of 17.8 dB.

The length of the pulse burst T_B, which is to equal the round-trip propagation time to the target, is given by

$$T_B = \frac{2R}{c} \tag{23}$$

where

c = the speed of light.

From this it follows that the number of pulses N in the burst is given by the product of the pulse-repetition frequency (PRF) and T_B. Each pulse in the burst is assumed to be modulated in order to improve the range resolution to 300.0 metres.

The radar sensor used in the baseline system is a uniformly-illuminated circular aperture of 70.0 metres in diameter for transmitting and receiving. The values for the remaining system parameters are as follows:

Peak Power (P_k) = 17.0 kW;
Pulse Length (τ) = 50.0 μsec (uncompressed);
Pulse Repetition Frequency (PRF) = 10 KHz;
System losses (L_s) = -9.0 dB;

System noise ($N_o = KT_s$) = -201.7 dB,

where

K is Boltzman's constant

and

T_s is the system noise temperature.

The system is required to detect the target out to a radar range R of at least 3.390×10^6 metres coresponding to a grazing angle $\gamma = 3.0°$. With these parameters the signal level S may be determined from the the standard radar equation

$$S = \frac{NP_k \tau G_c^2 \lambda^2 \sigma_T}{(4\pi)^3 R^4 L_s} \quad , \tag{24}$$

from which the signal-to-noise ratio (SNR) is determined:

$$SNR = \frac{S}{N_o} \quad . \tag{25}$$

There are N = 226 pulses per burst at this radar range. This value of N together with the remaining system parameters yield a signal-to-noise ratio (SNR), which is the signal-to-interference (SIR) in the absence of clutter that is greater than the minimum value of 17.8 dB thereby meeting the design criteria. Some parameters, such as noise temperature T_s, have been arbitrarily chosen, but reflect current technology. With this baseline system, other antenna systems may be used in place of that which was initially chosen with an appropriate adjustment in the peak power in order to keep the power density constant at the maximum of the antenna pattern.

6. SYSTEM PERFORMANCE IN THE PRESENCE OF EARTH-CLUTTER

In this section, results of the calculations of the signal-to-interference ratio (SIR) as a function of the relative velocity are presented for two cases; (1) a Taylor-weighted circular aperture for transmitting and receiving, and (2) a uniformly-illuminated circular aperture for transmitting and the same aperture but with Taylor weighting applied for receiving. Two values of the look-down angle θ_L, corresponding to grazing angles γ of 3.0° and 40.0°, are considered. For these examples the clutter-velocity spectrum is computed for two antenna orientations; ϕ_L = 0.0° corresponding to the look-ahead direction which is in line with the direction of motion of the satellite, and ϕ_L = 90.0° coresponding to a direction which is perpendicular to the direction of motion of the satellite. In these examples, the latitude of the satellite was set to δ_S = 90.0°, that is, the satellite was positioned over the geometric north pole; the clutter reflectivety was set to a constant value of -20.0 dBsm. Since the results are plots of the SIR against relative velocity, they serve to illustrate the detection performance of the SBR system in the presence of earth clutter as a function of the radial velocity component of the target in the radar's look direction.

The clutter level is computed by (a) identifying those clutter elements on the surface of the Earth which have the appropriate velocities that fall within the velocity bin of the signal processor, (b) weighting their levels according to the antenna responses in the directions at which they were identified, and (c) summing all those elemental contributions to determine the total contribution of earth clutter in the bin. The SIR is calculated by taking the ratio of the signal level to the addition of the noise and clutter levels.

In fig.(7), a plot is given of the SIR against velocity for γ = 3.0° and ϕ_L = 0.0° using the uniformly-illuminated circular aperture for transmitting and receiving. In this case, for velocities in excess of 26.0 m/sec, there is a clear area in the spectrum in which

the signal-to-interference ratio is limited only by system noise. This clear area arises because the earth-clutter elements with relative velocities greater than 26.0 m/sec lie in the radar shadow of the Earth. The dashed line in the figure represents the threshold detection level of 17.8 dB. Targets in which the SIR fall below this level are not detectable by the radar satellite. Note that targets having radial velocity components which fall inside the range from -132.0 m/sec to 24.0 m/sec are not detectable. These limits are defined as the Minimum Detectable Velocities (MDV) of the system for this look-direction.

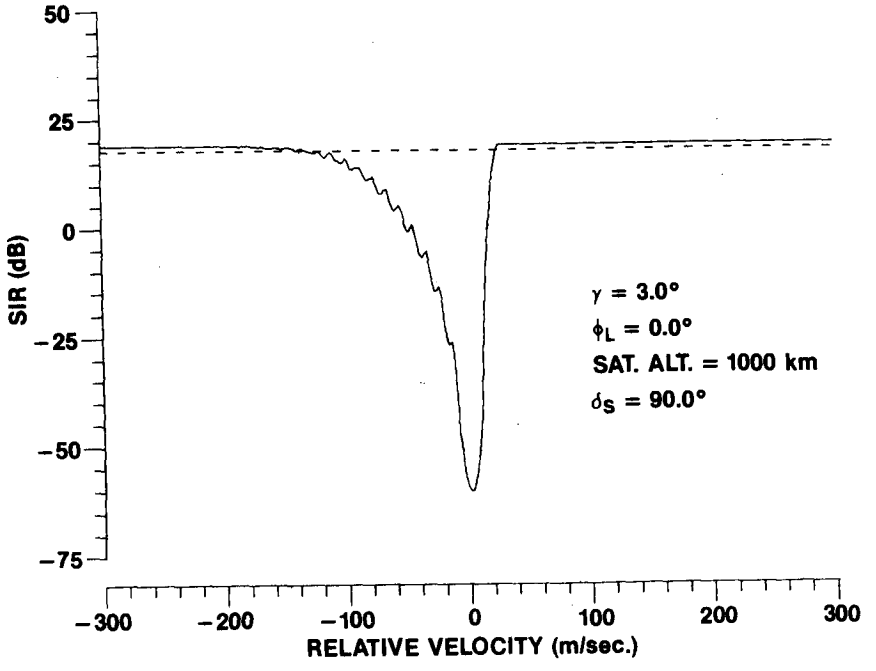

Figure 7 Plot of the SIR against velocity using a uniformly-illuminated circular aperture for transmitting and receiving.

In fig.(8), a plot is given of the SIR against velocity for the same look-direction as before but using a 40.0 dB Taylor-weighted circular aperture for transmitting and receiving. Again, there is a clear area in the spectrum in which the signal-to-interference ratio is limited only by system noise. Note that targets having radial velocity

components which fall inside the range from -62.0 m/sec to 18.0 m/sec are not detectable. These are the MDV which result when the weighted circular aperture is used in place of one that is uniformly-illuminated. It is evident from these results that Taylor weighting results in a significant reduction of the MDV because of the suppression of the clutter contributions in the sidelobes of the antenna pattern.

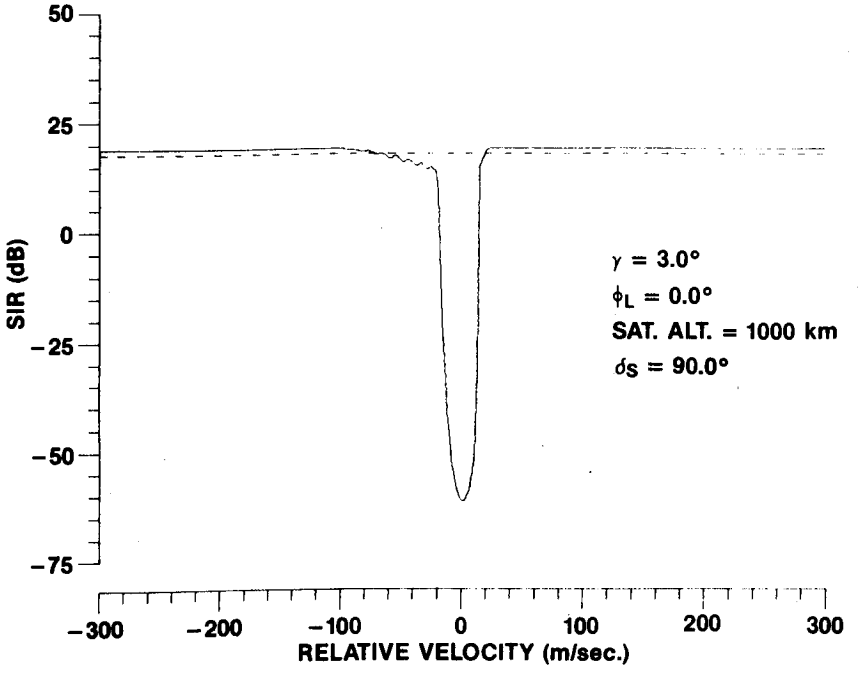

Figure 8 Plot of the SIR against velocity using a 40.0 dB Taylor-weighted circular aperture for transmitting and receiving.

In fig.(9), a plot is given of the SIR against velocity for $\gamma = 3.0°$ and $\phi_L = 90.0°$ using the uniformly-illuminated aperture for transmitting and receiving. This result differs considerably from that of fig.(7), in that there is now, no clear area in the spectrum. The SIR is now a symmetrical function of velocity. Note that targets with radial velocity components inside the range -270.0 m/sec to 270.0 m/sec are not detectable. These limits are the MDV of the system for this look-direction.

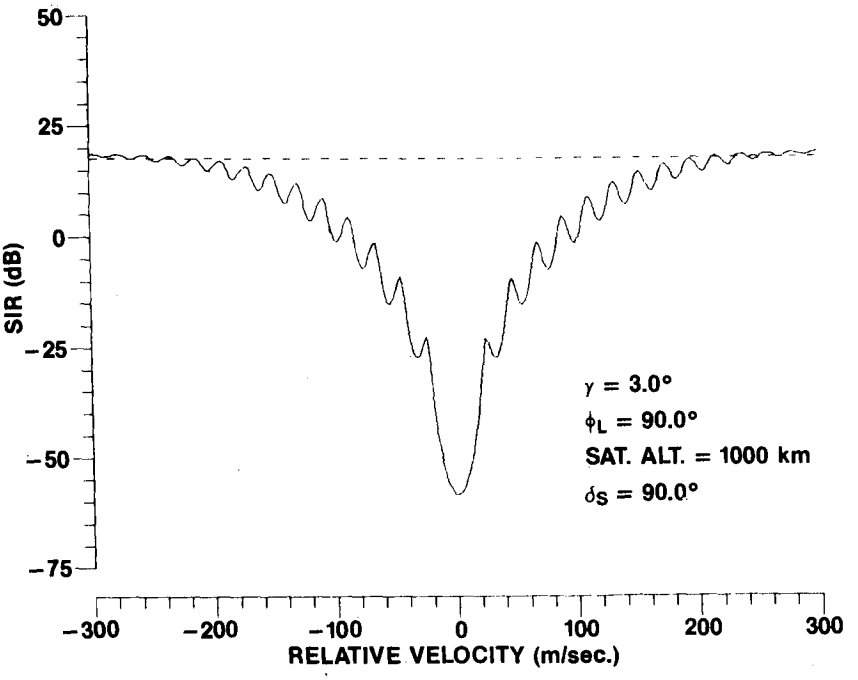

Figure 9 Plot of the SIR against velocity using a uniformly-illuminated circular aperture for transmitting and receiving.

In fig.(10), a plot is given of the SIR against velocity for $\gamma = 3.0°$ and $\phi_L = 90.0°$ using the circular aperture with 40.0 dB Taylor weighting applied. Again, Taylor weighting has reduced the MDV to ±122.0 m/sec. However, because of the side-looking aspect of the radar's look-direction, the clutter-velocity is spread and hence the MDV are greater than in the look-ahead direction shown in fig.(8).

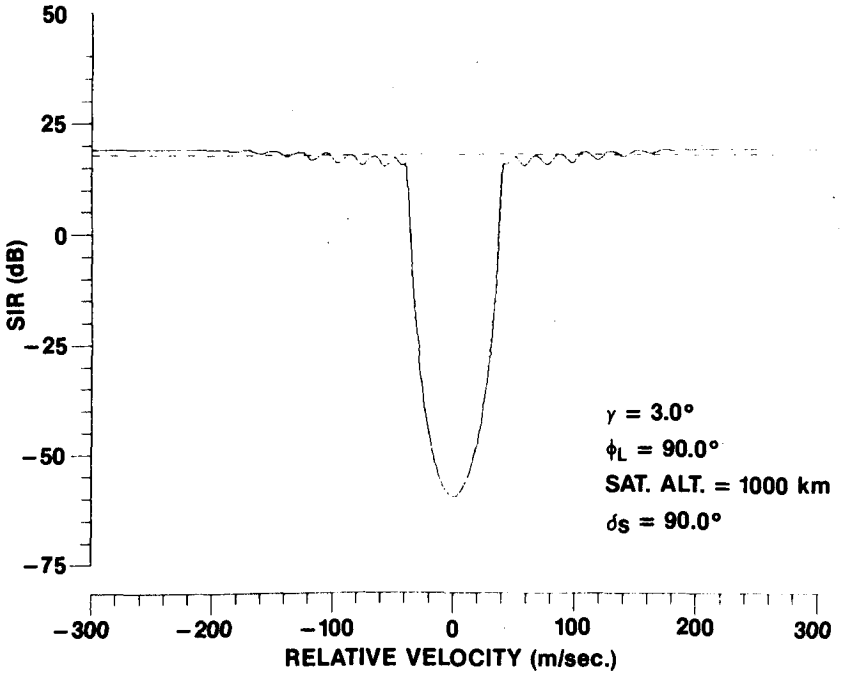

Figure 10 Plot of the SIR against velocity using a 40.0 dB Taylor-weighted circular aperture for transmitting and receiving.

As a further example of the effectiveness of Taylor weighting, fig.(11) shows a plot of the SIR against velocity for the same look-direction and antenna system which gave rise to the results of fig.(10), except that the SLR used was 45.0 dB. This result illustrates that the MDV, which are ±43.0 m/sec, are now limited by the width of the main lobe of the antenna pattern since the clutter contributions in the sidelobes have been reduced to negligible proportions. Any further reduction in the SLR will result in a broadening of the main lobe and a resultant increase in the MDV.

The results given in figs.(7) - (11) illustrate the extremes of the expected performance of the system at this grazing angle. For other values of ϕ_L, a partial filling in of the clear area arises together with an associated spread in the spectrum. This is illustrated in fig.(12), where plots are given of the MDV against ϕ_L for different values of SLR. The values of $\phi_L = 180.0°$ corresponds to the look-back direction which is a direction opposite to the direction of motion of

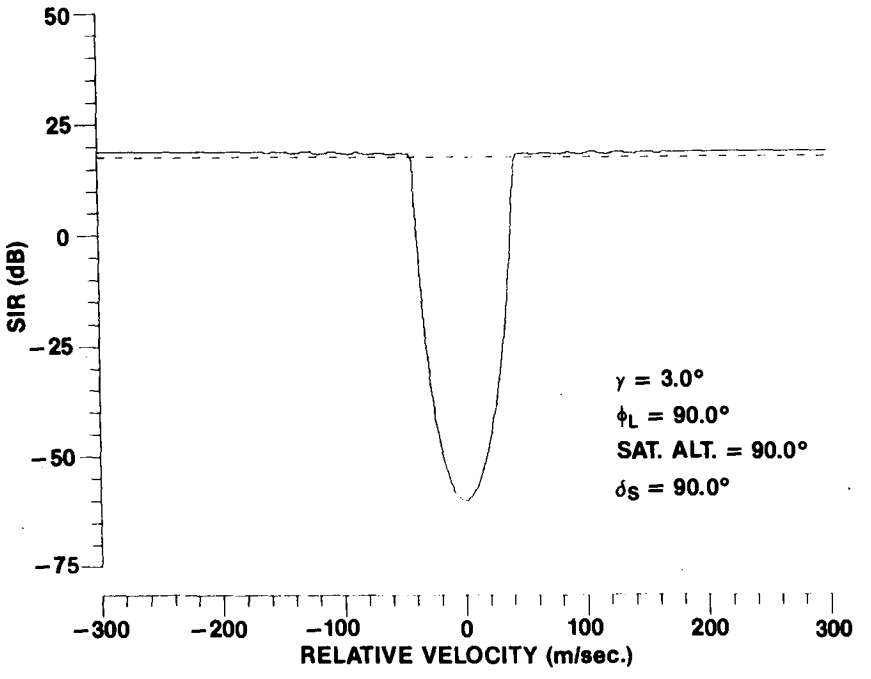

Figure 11 Plot of the SIR against velocity using a 45.0 dB Taylor-weighted circular aperture for transmitting and receiving.

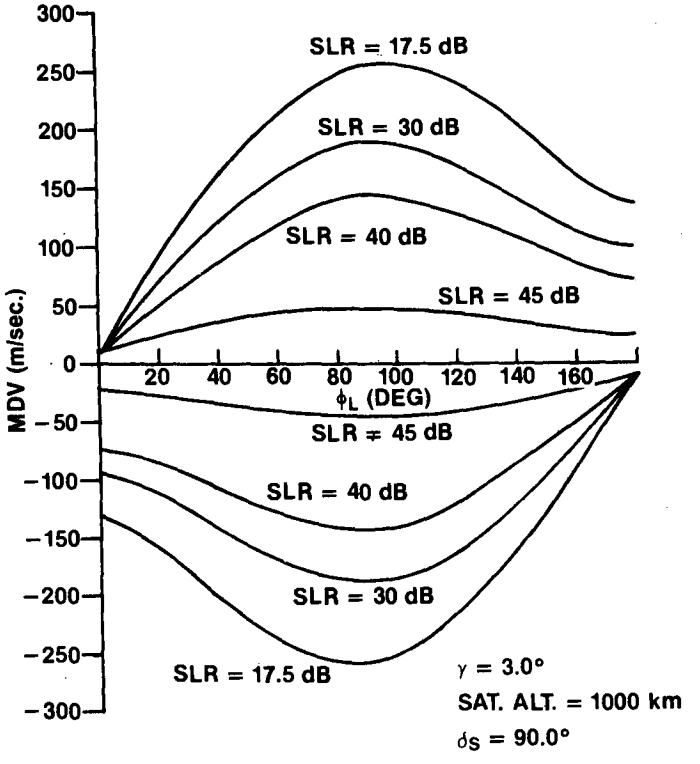

Figure 12 Plot of the MDV against ϕ_L for various values of SLR on transmit and receive.

the satellite. The value of SLR of 17.5 dB indicates that the antenna system used for transmitting and receiving was a uniformly-illuminated aperture. These results illustrate that the MDV decrease with increasing values of SLR. The curves for the MDV are skew symmetric about the ϕ_L axis with the minimum MDV occurring at ϕ_L = 0.0° or 180.0° (look-ahead or back), and the maximum occurring at ϕ_L = 90.0° (sideways looking).

For comparison, fig.(13) show plots of the MDV against ϕ_L for the same grazing angles as before but using an antenna system comprising a uniformly-illuminated circular aperture for transmitting and Taylor-weighted circular aperture for receiving. Again, it is noted that the values of the MDV decreased with increasing values of SLR. However, there is a noticeable degradation in the detection performance of this system compared to the system which gave rise to the results in fig.(12). This degraded performance arises as a result of the higher sidelobe levels in the antenna pattern when transmitting with a uniformly-illuminated aperture.

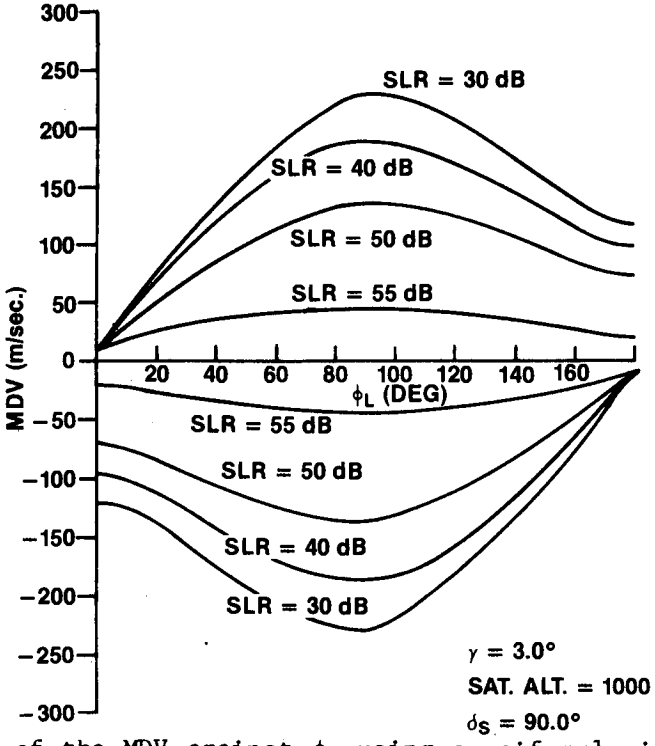

Figure 13 Plot of the MDV against ϕ_L using a uniformly-illuminated circular aperture for transmitting but for various values of SLR on receive.

The results given in figs.(12) - (13) illustrate that the worst detection performance occurs in the sideways looking direction (ϕ_L = 90.0°). Taking the worst case situation, and realizing that the values of the MDV are numerically the same at this look-azimuth angle, a new quantity, defined as the absolute maximum value of the Minimum Detectable Velocities, denoted $|MDV|_{max}$, may be used to quantify the detection performance of SBR systems. This is a useful quantity for this purpose since for a given look-down angle, detections are assured for all look-azimuth angles if the numerical values of the radial velocities considered equal or exceed $|MDV|_{max}$.

In fig.(14), plots are given of the $|MDV|_{max}$ as a function of the sidelobe-level ratio (SLR). The curve labelled (1) shows the result when an antenna system comprising a Taylor-weighted circular aperture is used for transmitting and receiving. The curve labelled (2) shows the result when the antenna system, comprising a uniformly-illuminated circular aperture for transmitting and the same aperture but with Taylor weighting applied for receiving is used. It is noted that the minimum value of $|MDV|_{max}$ occurs at an SLR of 45.0 dB for antenna system (1) and 55.0 dB for antenna system (2). It is also noted that for values of SLR greater than these, the detection performance decreases for both antenna systems. This decrease arises for the reasons explained earlier.

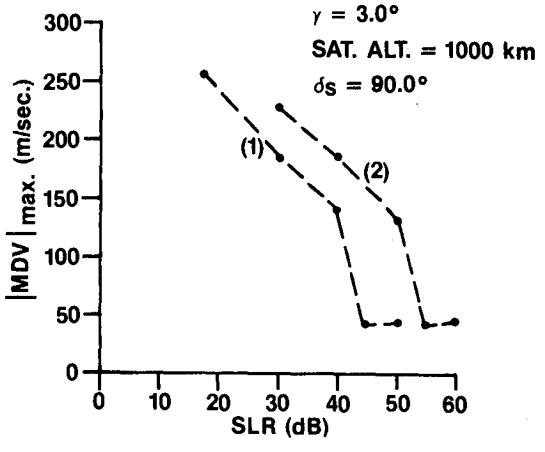

Figure 14 Plots of the absolute values of the maximum MDV against SLR.

In fig.(15), plots are given of the peak power required of the SBR system for the two antenna system considered, as a function of SLR. For example, antenna system (1) required a peak power of 38.3 kW when used with an SLR of 45.0 dB for optimum SBR detection performance. In comparison, antenna system (2) required 29.9 kW when used with an SLR of 55.0 dB for the same detection performance.

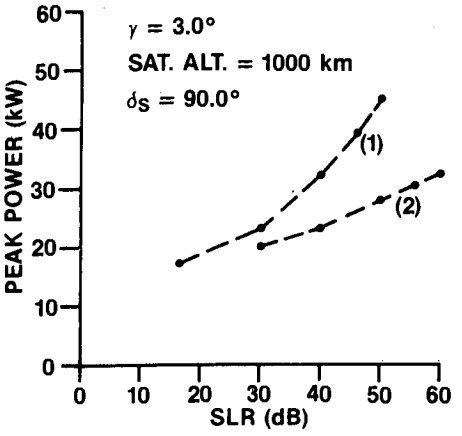

Figure 15 Plots of the peak power against SLR.

The best choice between (1) and (2) is not obvious since both present special difficulties to the radar systems engineer. In the case of (1), it may be quite difficult to achieve a Taylor-weighted transmission pattern with an active array without sacrificing efficiency in the element power modules. Antenna system (2) is more energy efficient than (1) but requires the achievement of a 55.0 dB reduction in the antenna sidelobes on reception as compared to 45.0 dB for (1). This requirement may be at or beyond the state of the art and will certainly require tighter mechanical and electrical tolerances than required for (1).

In the results which have been presented thus far only one grazing angle has been considered namely, $\gamma = 3.0°$. For greater values of γ an SBR will, in general, perform better because of the corresponding shorter radar ranges to the target (see eqn.(1)). As an example, fig.(16) shows a plot of the SIR against velocity for $\gamma = 40.0°$ and $\phi_L = 0.0°$

using the uniformly-illuminated circular aperture for transmitting and receiving. This result has a spiky appearance compared to that of fig.(7). The values of the MDV are difficult to determine in this result since the peaks of the curve cross over the threshold detection level several times. However, they might be considered to have values of -110.0 m/sec and 100.0 m/sec although the detection of smaller target velocities are possible.

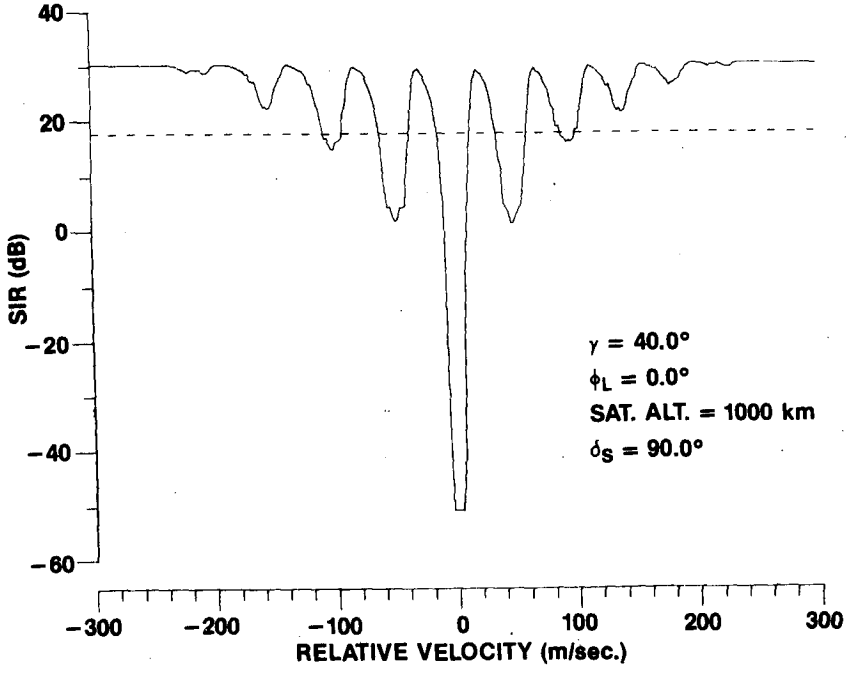

Figure 16 Plot of the SIR against velocity using a uniformly-illuminated circular aperture for transmitting and receiving.

This result is compared to that of fig.(17) where a 45.0 dB Taylor-weighted circular aperture was used for transmitting and receiving. Note that the MDV which are -6.0 m/sec and 5.0 m/sec, are considerably less than the values for the MDV of fig.(16).

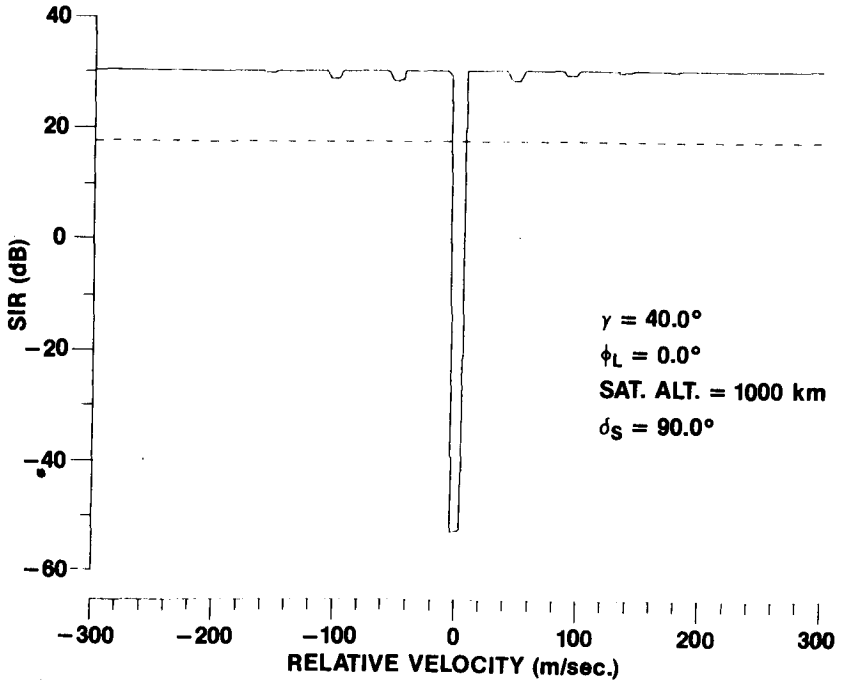

Figure 17 Plot of the SIR against velocity using a 45.0 dB Taylor-weighted circular aperture for transmitting and receiving.

In fig.(18), a plot is given of the SIR against velocity for $\gamma = 40.0°$ and $\phi_L = 90.0°$ using a uniformly-illuminated circular aperture for transmitting and receiving. The MDV for this result is ±110.0 m/sec, and illustrates the worst-case situation.

In fig.(19), a plot is given of the SIR against velocity for the same look-direction as above using a 45.0 dB Taylor-weighted circular aperture on transmit and receive. The MDV for this result is ±43.0 m/sec again illustrating, by comparison, the improvements in the detection performance of the system when aperture weighting is applied.

The improvements to be expected in the detection performance at other grazing angles when aperture weighting is applied, is illustrated

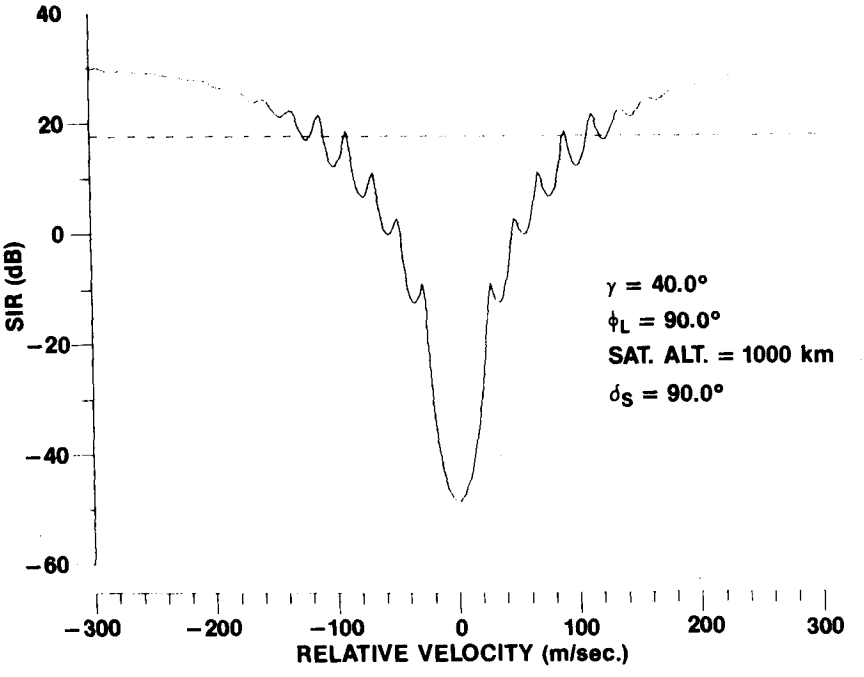

Figure 18 Plot of the SIR against velocity using a uniformly-illuminated circular aperture for transmitting and receiving.

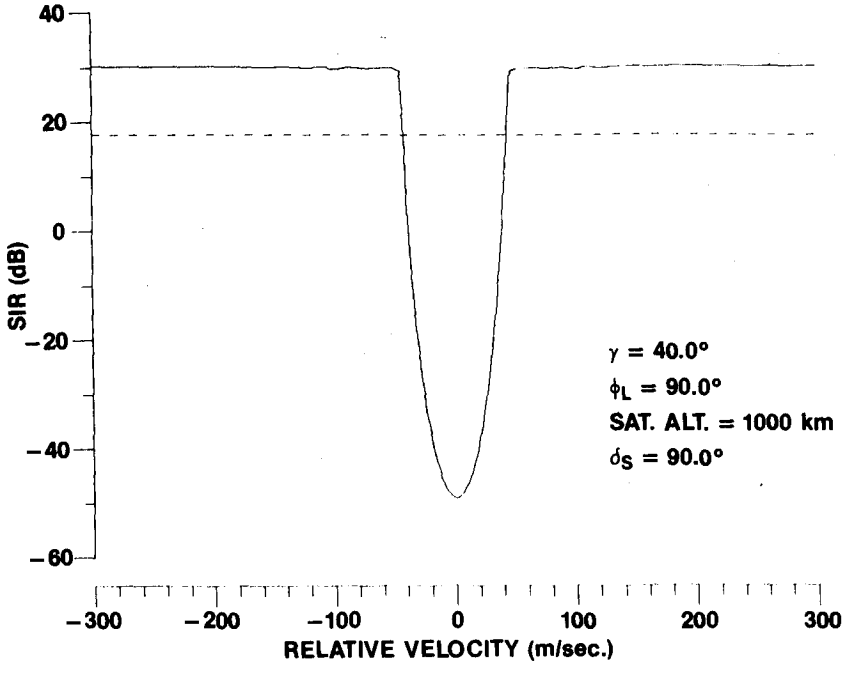

Figure 19 Plot of the SIR against velocity using a 45.0 dB Taylor-weighted circular aperture for transmitting and receiving.

in fig.(20). This figure show plots of the $|MDV|_{max}$ against grazing angle γ. The curve labelled A, illustrates that when a uniformly-illuminated circular aperture is used for transmitting and receiving, the detection performance improves with increasing γ. For comparison, the curve labelled B shows the resultant detection performance when antenna systems (1) and (2) are used with 45.0 dB and 55.0 dB Taylor weighting applied respectively. These values of SLR were chosen since they give the optimum SBR detection performance. Only one curve is shown for these two systems since both give the same results. The results exhibit a noticeable improvement in the performance compared with that which gave rise to curve A, and remain reasonably constant over the range of grazing angles considered. For grazing angles greater than those shown, the concept of a Minimum Detectable Velocity becomes less meaningful since the velocity component of the target in the radar's look-direction decreases to small values for grazing angles greater than these.

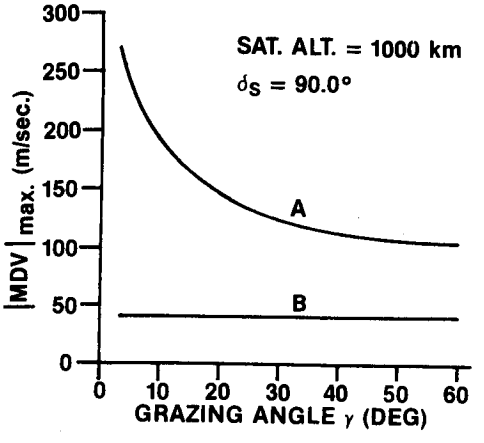

Figure 20 Plots of the $|MDV|_{max}$ against grazing angle γ, aperture diameter = 70.0m.

As further examples of system detection performance, fig.(21) shows a plot of the $|MDV|_{max}$ against aperture diameter at the 3.0° grazing angle using antenna system (1) with an SLR of 45.0 dB and antenna systems (2) with an SLR of 55.0 dB. Only one curve is plotted

in fig.(21) since the results from both these antenna systems are the same. It is noted that the $|MDV|_{max}$ decreases with increasing aperture diameter. This decrease arises because the main lobe of the antenna pattern is also decreasing with increasing aperture diameter.

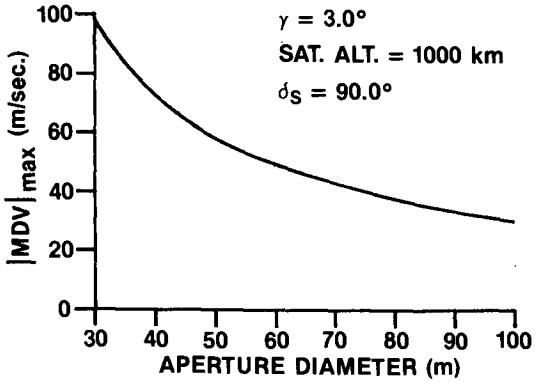

Figure 21 Plot of the $|MDV|_{max}$ against aperture diameter.

In Fig.(22), plots are given of the corresponding peak power required of the SBR system as a function of aperture diameter for the two antenna systems. The results show a rapid increase in the peak-power requirements with decreasing aperture diameter. The results given in figs.(21) - (22) clearly illustrate the need for large antenna apertures with sufficiently low sidelobe levels in SBR systems in order to keep the peak power to reasonable values, and to provide effective spatial discrimination against earth clutter.

In fig.(23), a plot is given of the $|MDV|_{max}$ against satellite altitude for the same grazing angle as before, using antenna systems (1) and (2) with a fixed aperture diameter of 70.0 metres. Again, there is only one curve in this figure since both antenna systems give the same results. It is noted that the $|MDV|_{max}$ slowly decreases with increasing satellite altitude. This slow decrease arises because of the opposing effects of increasing footprint size and decreasing satellite velocity with increasing altitude.

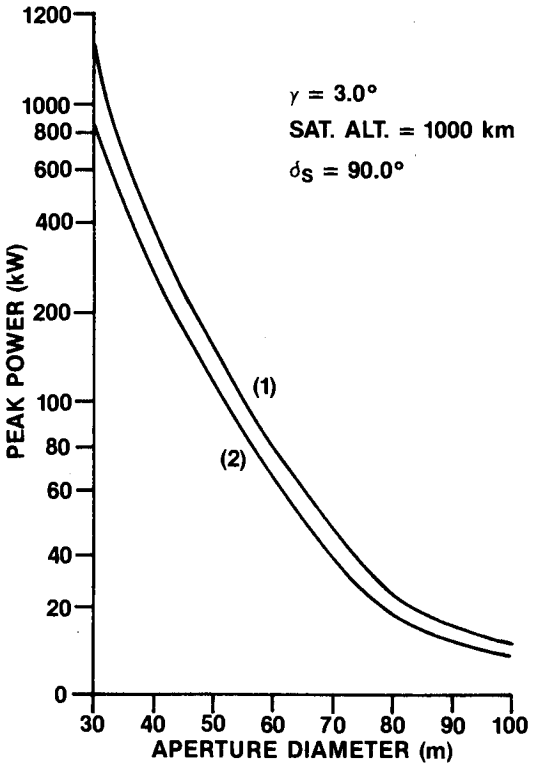

Figure 22 Plots of the peak power against aperture diameter.

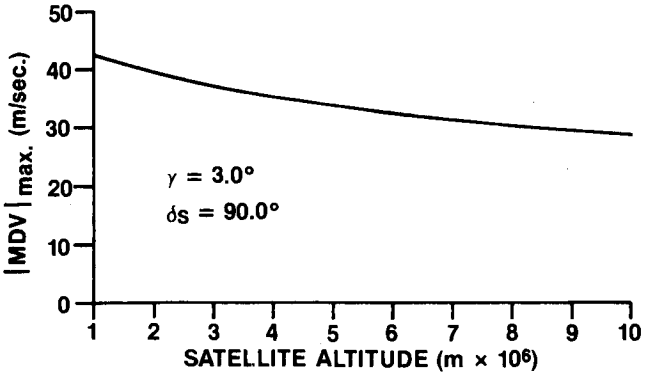

Figure 23 Plot of the $|MDV|_{max}$ against satellite altitude, aperture diameter = 70.0 m.

In fig.(24), plots are given of the corresponding peak power required of the SBR system to give a constant power density at the maximum of the antenna pattern for the two antenna systems. These results illustrate the dramatic increase in the peak power with increasing satellite altitude.

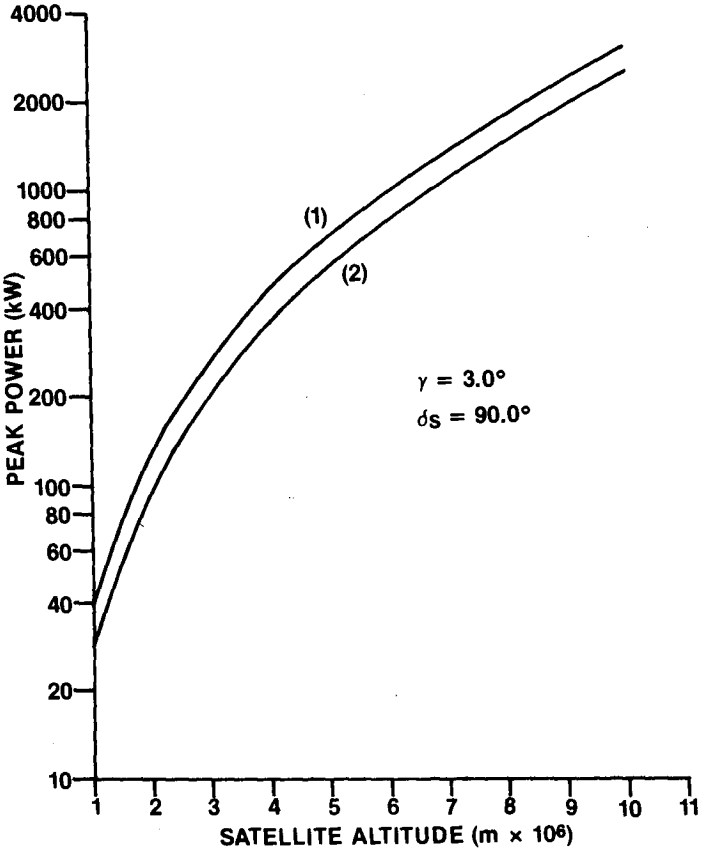

Figure 24 Plots of the peak power against satellite altitude, aperture diameter = 70.0m.

The results which have been presented in this section clearly illustrate that the detection performance of an SBR system can be greatly improved by the application of Taylor weighting to the antenna aperture. However, it should be kept in mind that this improvement is achieved at the expense of increasing the radar system's peak power.

From these results, one may well use the argument that since the improved performance has been brought about at the expense of increasing the peak power, then it seems reasonable to suppose that the same performance can be brought about by using the uniformly-illuminated aperture and increasing the peak power accordingly. However, it is not possible to achieve the same performance in this way because the corresponding radar system will become clutter limited at larger velocities due to the contributions of earth clutter entering through the higher antenna sidelobe levels. As an example of this, fig.(25) show plots of the SIR (solid line), and the signal-to-clutter ratio (SCR) shown by the dashed line, against velocity, for $\gamma = 3.0°$ and $\phi_L = 90.0°$ using the uniformly-illuminated circular aperture of 70.0 metres in diameter for transmitting and receiving, with a peak power of 38.3 kW. For these results, the satellite was positioned over the geometric north pole at an altitude of 1000 km. The detection performance of this system is quantified by the values of the MDV determined from the SIR curve; these values are ±190.0 m/sec. Note that the SIR curve converges to the SCR curve at velocities of ±150.0 m/sec. For velocities inside this range, defined as the clutter-limited region, both curves are identical indicating that they are independent of peak power. For velocities larger than these, the results are not independent of peak power, and hence a further increase in the system's peak power will result in a further reduction in the MDV. Thus, in the limit as the peak power approaches infinity, the MDV approaches that determined from the SCR curve. Therefore, the MDV determined from this curve quantify the limits of the detection performance of this system; these values are ±170.0 m/sec. Comparing this performance result to the result obtained in fig.(11) using the 45.0 dB Taylor-weighted aperture for transmitting and receiving, a stark contrast in the performances of the two systems is observed.

Thus, although in the results presented in this section, the peak power was adjusted accordingly to keep the power density constant so that direct comparisons could be made of the performances of the Taylor-weighted and uniformly-illuminated apertures, the important point

to realize from the results is that the weighted aperture provides a much better descrimination against earth clutter due to the suppression of the earth-clutter contributions in the sidelobes of the corresponding antenna pattern.

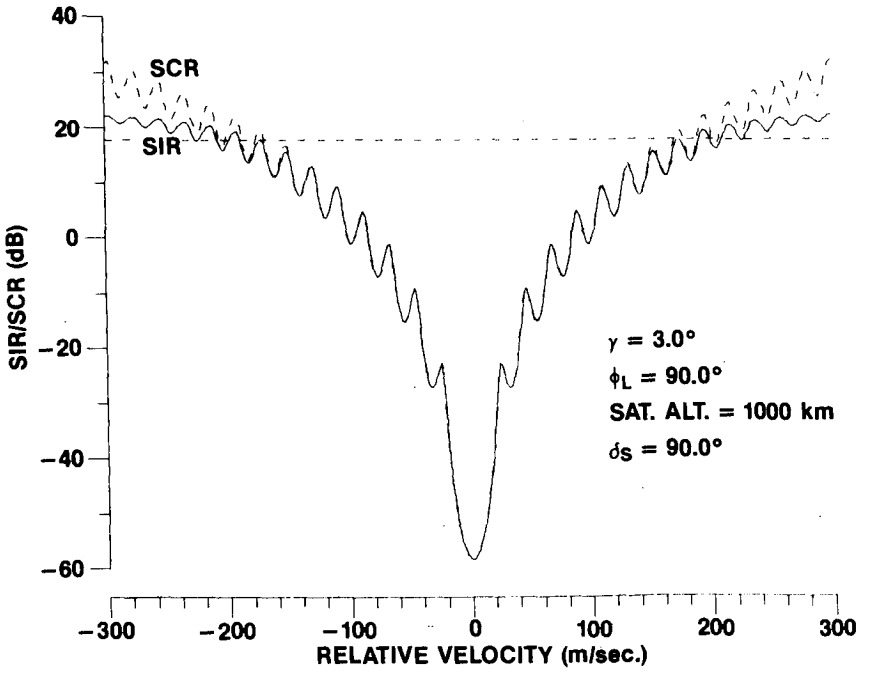

Figure 25 Plots of the signal-to-interference ratio (SIR) and signal-to-clutter ratio (SCR) against velocity.

Finally, in the results presented here, the latitude of the satellite was set to $\delta_s = 90.0°$, that is, the satellite was positioned over the geometric north pole. For other values of δ_s, the corresponding results differ only slightly from those presented here since the ground velocity of the satellite is so much greater than the velocity of the Earth[1].

7. SUMMARY AND CONCLUSION

Comparisons have been made of the detection performance of an SBR system using an antenna system comprising (1) a Taylor-weighted circular

aperture for transmitting and receiving, and (2) a uniformly-illuminated aperture for tansmitting and the same aperture but with Taylor weighting applied for receiving.

The results of these studies show that, in general, with the application of Taylor weighting to the antenna aperture, a marked improvement in the detection performance of an SBR system can be achieved. In addition, the results from the comparative studies show that when antenna system (1) was used, the SBR detection performance was at its optimum when the antenna aperture was weighted according to 45.0 dB Taylor weighting, whereas when antenna system (2) was used, 55.0 dB Taylor weighting was required to arrive at the same optimum performance.

8. ACKNOWLEDGEMENT

This work was sponsored by the Department of National Defence, Canada.

9. REFERENCES

1] Rook, B.J., J.S. Bird and A.W. Bridgewater, "Detection of Near-Earth Targets by Space-Based Radar: Development and Use of Computer Simulations", CRC Report 1389, July 1985, Ottawa, Canada.

2] Skolnik, M.I., "Introduction to Radar Systems", McGraw-Hill Book Company, 1962, p.326.

3] Taylor, T.T., "Design of Line-source Antennas for Narrow Beamwidth and Low Sidelobes", IRE TRANS. on Antenna and Propagation, Vol. AP-3, pp.16-28, January 1955.

4] Taylor, T.T., "Design of Circular Apertures for Narrow Beamwidth and Low Sidelobes", IRE TRANS. Vol. AP8, January 1960, No. 1, pp.17-27.

5] Rudge, A.W., K. Milne, A.D. Olver and P. Knight, "The Handbook of Antenna Design", Vol. 2, 1983: Peter Peregrinus Ltd., Lond. UK, pp.156-157.

6] Rudduck, R.C., et al, "Directive Gain of Circular Taylor Patterns", Radio Science, Vol. 6, No. 12, pp.1117-1121, December 1971.

UNCLASSIFIED
Security Classification

DOCUMENT CONTROL DATA - R & D
(Security classification of title, body of abstract and indexing annotation must be entered when the overall document is classified)

1 ORIGINATING ACTIVITY
Defence Research Establishment Ottawa
Department of National Defence
Ottawa, Ontario, K1A 0Z4

2a. DOCUMENT SECURITY CLASSIFICATION
UNCLASSIFIED

2b. GROUP

3. DOCUMENT TITLE
Comparisons of the Detection Performance of a Space-Based Radar System Using Different Antenna Systems and Aperture Illuminations

4 DESCRIPTIVE NOTES (Type of report and inclusive dates)
CRC Report

5. AUTHOR(S) (Last name, first name, middle initial)
ROOK, B.J.

6. DOCUMENT DATE	7a. TOTAL NO. OF PAGES	7b. NO. OF REFS
May 1986	40	6

8a. PROJECT OR GRANT NO.	9a. ORIGINATOR'S DOCUMENT NUMBER(S)
33C87	CRC Report No. 1401
8b. CONTRACT NO.	9b. OTHER DOCUMENT NO.(S) (Any other numbers that may be assigned this document)

10. DISTRIBUTION STATEMENT
Unlimited

11. SUPPLEMENTARY NOTES	12. SPONSORING ACTIVITY

13. ABSTRACT

Comparisons have been made of the results of the detection performance of a space-based radar (SBR) system using uniformly-illuminated circular apertures, and the same apertures with Taylor weighting applied. From the studies, it is shown that the detection performance of an SBR system can be greatly improved with the application of the latter form of weighting.

For the comparative studies, two antenna systems with the same physical dimensions were used, (1) a Taylor-weighted circular aperture for transmitting and receiving, and (2) a uniformly-illuminated circular aperture for transmitting, and the same aperture but with Taylor weighting applied for receiving. These comparative studies show that when antenna system (1) was used, 45.0 dB Taylor weighting was required in order to achieve the optimum SBR detection performance whereas for antenna system (2), 55.0 dB was required to give the same detection performance.

UNCLASSIFIED
Security Classification

KEY WOROS

Space

Based

Radar

INSTRUCTIONS

1. ORIGINATING ACTIVITY: Enter the name and address of the organization issuing the document.

2a. DOCUMENT SECURITY CLASSIFICATION: Enter the overall security classification of the document including special warning terms whenever applicable.

2b. GROUP: Enter security reclassification group number. The three groups are defined in Appendix 'M' of the DRB Security Regulations.

3. DOCUMENT TITLE: Enter the complete document title in all capital letters. Titles in all cases should be unclassified. If a sufficiently descriptive title cannot be selected without classification, show title classification with the usual one-capital-letter abbreviation in parentheses immediately following the title.

4. DESCRIPTIVE NOTES: Enter the category of document, e.g. technical report, technical note or technical letter. If appropriate, enter the type of document, e.g. interim, progress, summary, annual or final. Give the inclusive dates when a specific reporting period is covered.

5. AUTHOR(S): Enter the name(s) of author(s) as shown on or in the document. Enter last name, first name, middle initial. If military, show rank. The name of the principal author is an absolute minimum requirement.

6. DOCUMENT DATE: Enter the date (month, year) of Establishment approval for publication of the document.

7a. TOTAL NUMBER OF PAGES: The total page count should follow normal pagination procedures, i.e., enter the number of pages containing information.

7b. NUMBER OF REFERENCES: Enter the total number of references cited in the document.

8a. PROJECT OR GRANT NUMBER: If appropriate, enter the applicable research and development project or grant number under which the document was written.

8b. CONTRACT NUMBER: If appropriate, enter the applicable number under which the document was written.

9a. ORIGINATOR'S DOCUMENT NUMBER(S): Enter the official document number by which the document will be identified and controlled by the originating activity. This number must be unique to this document.

9b. OTHER DOCUMENT NUMBER(S): If the document has been assigned any other document numbers (either by the originator or by the sponsor), also enter this number(s).

10. DISTRIBUTION STATEMENT: Enter any limitations on further dissemination of the document, other than those imposed by security classification, using standard statements such as:

(1) "Qualified requesters may obtain copies of this document from their defence documentation center."

(2) "Announcement and dissemination of this document is not authorized without prior approval from originating activity."

11. SUPPLEMENTARY NOTES: Use for additional explanatory notes.

12. SPONSORING ACTIVITY: Enter the name of the departmental project office or laboratory sponsoring the research and development. Include address.

13. ABSTRACT: Enter an abstract giving a brief and factual summary of the document, even though it may also appear elsewhere in the body of the document itself. It is highly desirable that the abstract of classified documents be unclassified. Each paragraph of the abstract shall end with an indication of the security classification of the information in the paragraph (unless the document itself is unclassified) represented as (TS), (S), (C), (R), or (U).

The length of the abstract should be limited to 20 single-spaced standard typewritten lines; 7½ inches long.

14. KEY WORDS: Key words are technically meaningful terms or short phrases that characterize a document and could be helpful in cataloging the document. Key words should be selected so that no security classification is required. Identifiers, such as equipment model designation, trade name, military project code name, geographic location, may be used as key words but will be followed by an indication of technical context.